Generation of Isomers for Icosahedral Clusters $A_{12-x}B_x$ (x = 0 – 12) from a Symmetry-Based Algorithm

Stefan Knoppe

Molecular Imaging and Photonics, Department of Chemistry, KU Leuven, Celestijnenlaan 200D, 3001 Heverlee, Belgium

stefan.knoppe@chem.kuleuven.be

Abstract

All isomers of (quasi-)icosahedral, binary $A_{12-x}B_x$ clusters were constructed based on a simple symmetry-base algorithm. This algorithm can also be applied to other starting geometries, but it is advantageous to restrict to high starting symmetries and high degeneracies of atom sites. Also, the (relative) degeneracies of the isomers are calculated. Chiral isomers are identified, showing that chirality in binary, (quasi-)icosahedral clusters may play an important role in A_8B_4, A_7B_5, A_6B_6, A_5B_7, and A_4B_8. Chirality is of importance in nonlinear optics and asymmetric catalysis. The results provided may stimulate further research in these areas using binary metal clusters.

Table of Contents Figure and Synopsis

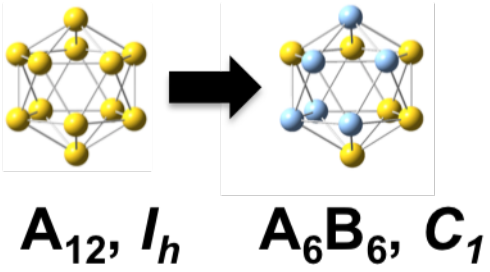

The geometrical isomers of (quasi)-icosahedral clusters $A_{12-x}B_x$ were constructed using group theoretical arguments. The degeneracies and chirality of the isomers were analyzed, showing that chirality becomes important at doping with four or more foreign atoms.

Introduction

Metal clusters M_m are widely studied in both physics and chemistry. This is due to their intriguing, size- and structure-dependent properties,[1–4] which give rise to interesting optical, magnetic and electronic effects. These are of interest in applications as contrast agents in imaging,[5–8] catalysis,[9,10] sensing,[7] but also in answering questions in metallurgy, e.g. how many atoms must be present to observe metallic behavior? The continuing interest in metallic clusters is also partly owed to their fascinating structures, which often are derived from regular polyhedra, such as icosahedra, dodecahedra, cuboctahedra, etc ….

The properties of a metal cluster M_m can be drastically altered when substituting one or several of the atoms by a foreign metal.[11] This gives rise to clusters $M_{m-x}M'_x$ (for convenience, we will use A for M and B for M' in the following). Continuous substitution, however, leads to a manifold of different isomers, which rapidly increase with the number of substitutions. For instance, the icosahedral A_{12} cluster has 12 equivalent atoms, which are located at the vertex sites of the icosahedron. Thus, substitution with one foreign atom B leads to one isomer $A_{11}B_1$. The second substitution gives three isomers of $A_{10}B_2$. In the next generation, $Au_{10}B_3$, a manifold of isomers is to be expected. The identification of these is not straightforward, since different starting isomers may yield the same structure. It is intuitive to assume that the situation is even more complicated for higher generations of substitution.

Dass and co-workers recently presented the x-ray crystal structure of Ag-doped $Au_{25}(SR)_{18}$ clusters (SR: thiolate).[12] The crystal structure determination yielded an average of 6.7 Ag atoms in all clusters, and the mass spectrometric analysis lead to a value of 6.2. From the mass spectra, it is obvious, that a mixture of clusters $Au_{25-x}Ag_x(SR)_{18}$ was obtained, with x ranging from 4 to 8. The basics structural features of the parent $Au_{25}(SR)_{18}$ cluster[13] are maintained: The cluster is composed of an icosahedral Au_{13} core (with a central atom), and the core is protected by six SR-(Au-SR)$_2$ motifs. The Ag atoms are located on the surface of the icosahedral core. This is in agreement with prior simulations, which predict this occupational behavior for doping thiolate-protected Au clusters with Ag.[14,15] Thus, the problem of isomerism can be reduced to the surface atoms of the $Au_{13-x}Ag_x$ core. Note that this substitution on the surface of the cluster core is unique to silver, e.g. palladium doping leads to substitution of the central atom.[16] Copper seems to occupy binding sites in the protecting SR-(Au-SR)$_n$ motifs.[17]

Along with the determination of the crystal structure of $Au_{25-x}Ag_x(SR)_{18}$, a density-functional theory (DFT) analysis of the Ag-doped clusters was provided.[12] Since the clusters co-crystallize in the same crystal, the data (and even less so mass spectrometry) do not provide information about the exact location of the Ag atoms and the distribution of the possible isomers for each substitution step. Instead, the crystal structure provides information about average Ag population of a specific site in the cluster. From this average population, a realistic and an artificial isomer of $Au_{19}Ag_6(SR)_{18}$ (which shows high abundance in the mass spectrum) was analyzed by means of DFT. Calculated absorption spectra of the two structures highlight the importance of the position of the Ag atoms in the doped Au cluster. However, a full theoretical analysis of all possible isomers of $Au_{19}Ag_6(SR)_{18}$ was not carried out. It should be mentioned that a vast number of isomers would have to be constructed and analyzed by DFT, which would lead to immense demand of computational resources. The occupation of surface sites in the $Au_{13-x}Ag_x$ centered, quasi-icosahedral cluster has also been observed in early crystallographic work by Teo et al. on silver-doped phosphine-protected Au clusters ('clusters of clusters'). Bi- and triicosahedral clusters were analyzed crystallographically, and in all cases the central atom of the icosahedral building blocks was occupied by an Au atom.[18–20] A bi-icosahedral binary kernel has also been observed in the crystal structure of $Au_{38-x}Ag_x(SR)_{24}$.[21]

The crystal structure of $Au_{25-x}Ag_x(SR)_{18}$ raises the question, how many geometric isomers are possible when the atoms of an icosahedral cluster A_{12} are subsequently substituted by foreign atoms B. To my knowledge, a thorough analysis of this problem has not been carried out to date. The position of foreign metals in clusters of high symmetry has implications on the point group symmetry of the obtained isomers. This is of particular importance in nonlinear optics, where second-order optical effects show a drastic dependence on the molecular symmetry.[22]

Another prominent candidate for doping is the icosahedral Al_{13} cluster.[23] The cluster has characteristics of a 'super-halogen' and is easily reduced to the anionic species, which leads to 40-electron shell closing ($1S^2\ 1P^6\ 1D^{10}\ 2S^2\ 1F^{14}\ 2P^6$ in the superatomic picture). Doping of the cluster with foreign atoms has been discussed, but only cases of up to $Al_{11}M_2$ were considered.[24–27] The fact that the Al_{13} superatom can be (isoelectronically) doped by foreign atoms, however, justifies the search for isomers of higher substitution.

A prominent related problem is that of the isomers of heterofullerenes. In these, carbon atoms in the C_n cage are substituted by foreign atoms, such as N, P, B, and (B,N).[28–32] Especially in the case of isoelectronically (B,N)-substituted fullerenes, a broad variety of possible isomers has to be considered. In a classic example, $C_{60-2x}(BN)_x$ (x = 1 - 7) was investigated by Pattanayak et al., making use of two-dimensional representations of the fullerenes (Schlegel diagrams).[30]

The aim of this article is to provide an overview of all possible isomers for foreign atom doped (quasi-)icosahedral clusters. We restrict ourselves to binary systems $A_{m-x}B_x$. The strategy presented here is entirely based on symmetry arguments and does not provide information of the relative stability of the isomers. The algorithm is generic and can be applied to all types of clusters, although a high symmetry (I_h, T_d, O_h, …) in the starting cluster is desirable. Johnson et al. have outlined the approach used here when considering potential isomers of $Fe_3(CO)_{12-x}(PR_3)_x$ clusters (up to x = 3).[33] In the $Fe_3(CO)_{12}$ cluster, a Fe_3 triangle is protected by twelve carbonyl ligands which adopt an icosahedral coordination geometry. The first generations in binary $A_{20-x}B_x$ of tetrahedral geometry are outlined as well.

Method

Quasi-icosahedral clusters $A_{12-x}B_x$ are discussed for x = 0 - 6. For x > 6, the same isomers are obtained as for x < 6, except that all atoms A are replaced by B and all atoms B are replaced by A. The nomenclature is as follows: each substitution leads to a new 'generation' $G^{(x)}$, e.g. A_{12} is $G^{(0)}$, $A_{11}B_1$ is $G^{(1)}$, $A_{10}B_2$ is $G^{(2)}$, etc …. Within each generation, the isomers are labeled as Ia, Ib, etc …. For instance, the three isomers of $G^{(2)}$ are $G^{(2)}$-Ia, $G^{(2)}$-Ib, and $G^{(2)}$-Ic (in analogy to carboranes these could also be labeled as *ortho*-, *meta*- and *para*-$Au_{10}B_2$,[34] yet, this nomenclature fails for x > 2). For each isomer, the molecular point group is determined. We start from an ideal icosahedron A_{12} with the point group I_h. Upon substitution, only the atom labels are changed (A is replaced by B), and all bond lengths and angles are kept constant. This constraint is for convenience, however, it should be pointed out that relaxation of the structures (e.g. by DFT) may lead to deviations from this idealized *quasi*-icosahedral geometry.[24]

After determination of the point group for each isomer, the remaining 12-x atoms A in the cluster $A_{12-x}B_x$ are grouped according to their symmetry equivalency. Optical isomers are treated as identical. The optical isomers will be identified individually at a

later stage to provide an overview of potential sources of chirality in binary, quasi-icosahedral $Au_{12-x}B_x$ clusters.

The degeneracy *g* of the isomers was determined as well (see below). The degeneracy and symmetry equivalencies are appended to the point group symbol, e.g. $G^{(2)}$-Ia-C_{2v}(60/3*2, 1*4) means: Isomer Ia of generation $G^{(2)}$ has the molecular point group C_{2v}, is 60-fold degenerate and the remaining ten atoms of A split into four sets (three times two equivalent atoms and one set of four equivalent atoms). This corresponds to either *ortho*- or *meta*-$Au_{10}B_2$. This example is discussed in detail below.

The degeneracy of each isomer is determined as follows: The parent icosahedral cluster A_{12} has a degeneracy of 1 (only one isomer). In $G^{(1)}$, only one isomer is found as well, but since each of the twelve atoms in A_{12} can be substituted, its degeneracy is 12, and the full descriptor is $G^{(1)}$-C_{5v}(12/2*5, 1*1). In $G^{(2)}$, three distinct isomers are obtained, since three groups of equivalent atoms can be substituted. The degeneracy of the isomers in $G^{(2)}$ is determined by which atom group in $G^{(1)}$ is substituted. In two of the cases, the atom groups consist of five atoms, and in the third case, only one atom can be substituted. The degeneracy of the isomers is therefore the degeneracy of the parent isomer multiplied by the number of equivalent atoms of which one is substituted. Hence, the isomers $G^{(2)}$-Ia and $G^{(2)}$-Ib have degeneracies of 60 (=12 * 5), and $G^{(2)}$-Ic is 12-fold degenerated (12 * 1). In general, the degeneracy of a new isomer is the degeneracy of the parent isomer multiplied by how many atoms are available for symmetry equivalent substitution. Note that the sum of the degeneracies of all isomers in each generation $G^{(x)}$ is:

$$g\left(G^{(x)}\right) = g\left(G^{(x-1)}\right) * \left(12 - (x-1)\right)$$

where $g(G^{(x)})$, $g(G^{(x-1)})$: total degeneracies of generations $G^{(x)}$ and $G^{(x-1)}$. The total degeneracies for each generation are listed in Table 1 for reference. They serve as test for the correct construction of isomers.

Table 1. Expected total degeneracies of each generation $G^{(x)}$ in (quasi-)icosahedral $A_{12-x}B_x$.

Cluster	G(x)	G(G(x))
A_{12}	0	1
$A_{11}B_1$	1	12
$A_{10}B_2$	2	132
A_9B_3	3	1320

A_8B_4	4	11880
A_7B_5	5	95040
A_6B_6	6	665280

We also introduce 'preliminary' denominators I1, I2, I3, etc … for the obtained isomers of each generation $G^{(x)}$. These preliminary isomers are generated from the individual isomers of $G^{(x-1)}$. For instance, $G^{(2)}$-Ia, $G^{(2)}$-Ib, and $G^{(2)}$-Ic lead to four, four and one new isomer in $G^{(3)}$, respectively. These nine isomers can be combined, since three of the isomers generated from $G^{(2)}$-Ib are identical to those generated from $G^{(2)}$-Ia (hence, $G^{(2)}$-Ib only leads to one new isomer). In addition, the isomer generated from $G^{(2)}$-Ic is identical to an isomer from $G^{(2)}$-Ia. In total, $G^{(2)}$ leads to five new isomers in $G^{(3)}$. When combining two identical isomers in the same generation (obtained from different isomers in the previous generation), their degeneracies add up. This strategy will become clear when examining each individual case (*vide infra*). The degeneracy of an isomer indicates how many individual ways can be used to generate a distinct isomer. The relative degeneracies of the isomers within one generation are calculated as well. This is important when calculating a property (e.g. the absorption spectrum) of each isomer and subsequent linear combination of these to predict the average absorption spectrum of one generation. For this, the population of each isomer has to be known, which can be achieved via a Boltzmann distribution. The factors that determine the population of each isomer are the relative energies of the isomers, and their degeneracies (and the temperature).

Results and Discussion

We begin the discussion with testing the algorithm for the (quasi-)octahedral $A_{6-x}B_x$ system. This is a well-known case in transition metal chemistry where thousands of examples of octahedral coordination spheres (complexes of the form ML_6-xL'_x) exist.[35] The isomers obtained from substituting the ligands in an octahedral coordination sphere (or atoms in an octahedral cluster) are limited and they are obtained straightforwardly. However, this is worked out in detail at this point to demonstrate the algorithm used.

We begin with octahedral A_6 (Figure 1). The point group is O_h and all atoms are equivalent ($G^{(0)}$-Ia-O_h(1/1*6). The substitution product is A_5B_1, the point group is C_{4v} and the remaining five atoms split into a set of four equivalent atoms and one remaining atom. The degeneracy is six, since replacement of any atom in $G^{(0)}$-Ia leads

to the same isomer. Thus, the full descriptor is $G^{(1)}$-Ia-C_{4v}(6/1*4, 1*1). Since the remaining five atoms split into two sets, two isomers must be possible in $G^{(2)}$. These are $G^{(2)}$-Ia-D_{4h}(6/1*4) (as in *trans*-$ML_4L'_2$) and G(2)-Ib-D_{2v}(24/2*2) (*cis*-$ML_4L'_2$). From $G^{(2)}$-Ib, one isomer can be obtained (with C_{2v} point group); two isomers can be constructed (with C_{2v} and C_{3v} symmetry). Inspection of the C_{2v} isomers shows that these are identical, hence, only two distinct isomers are obtained in $G^{(3)}$ (*mer*- and *fac*-$ML_3L'_3$). The isomers obtained by subsequent substitution of atoms in octahedral A_6 up to the third generation are shown in Figure 1. The characteristics of the isomers are shown in Table 2. In $G^{(4)}$, the same isomers as for $G^{(2)}$ are obtained, except that the atom types are reversed (A becomes B and B becomes A). This simple example demonstrates the algorithm employed here and the notations used in the following.

Table 2. Isomers and their characteristics for (quasi-)octahedral $A_{6-x}B_x$ (x = 0, 1, 2, 3) clusters.

Cluster	$G^{(x)}$	Number of Isomers	Point group	Rel. Degeneracy	Full Descriptor
A_6	$G^{(0)}$	1	O_h	1	O_h(1/1*6)
A_5B_1	$G^{(1)}$	1	C_{4v}	1	C_{4v}(6/1*4,1*1)
A_4B_2	$G^{(2)}$	2	D_{4h}	1	D_{4h}(6/1*4)
			C_{2v}	4	C_{2v}(24/2*2)
A_3B_3	$G^{(3)}$	2	C_{2v}	3	C_{2v}(72/1*2, 1*1)
			C_{3v}	2	C_{3v}(48/1*3)

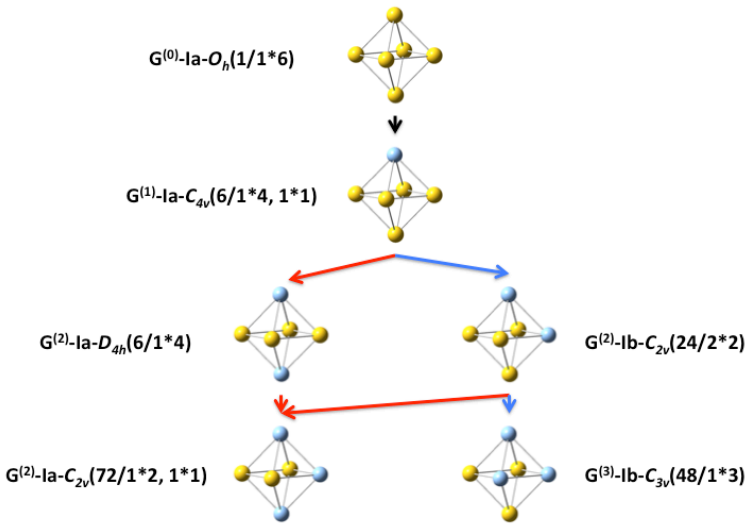

Figure 1. Isomers and geometric characteristics of (quasi-)octahedral $A_{6-x}B_x$ clusters for x = 0, 1, 2, and 3. The relationships between the isomers in $G^{(x)}$ and $G^{(x-1)}$ are indicated by arrows.

We now turn our focus to the isomers of the (quasi-)icosahedral $A_{12-x}B_x$ family. The construction of isomers of $G^{(0)}$, $G^{(1)}$, and $G^{(2)}$ is straightforward (Table 3, Figure 2). The ideal icosahedron A_{12} has twelve equivalent sites with can be substituted to generate $G^{(1)}$. The single isomer in $G^{(1)}$ has three groups of atoms, consisting of five, five, and one, respectively. This leads to three isomers in $G^{(2)}$ with a degeneracy of 60:60:12 (relative degeneracy 5:5:1). Note that the point group for $G^{(2)}$-Ia and $G^{(2)}$-Ib is identical, yet, the cluster structures are not.

Table 3. Isomers of $G^{(0)}$ (A_{12}), $G^{(1)}$ ($A_{11}B_1$) and $G^{(2)}$ ($A_{10}B_2$), their point groups and degeneracies.

Cluster	$G^{(x)}$	Number of Isomers	Point group	Rel. Degeneracy	Full Descriptor
A_{12}	$G^{(0)}$	1	I_h	1	I_h(1/1*12)
$A_{11}B_1$	$G^{(1)}$	1	C_{5v}	1	C_{5v}(12/2*5,1)
$A_{10}B_2$	$G^{(2)}$	3	C_{2v}	5	C_{2v}(60/1*4, 3*2)
			C_{2v}	5	C_{2v}(60/1*4, 3*2)
			D_{5d}	1	D_{5d}(12/1*10)

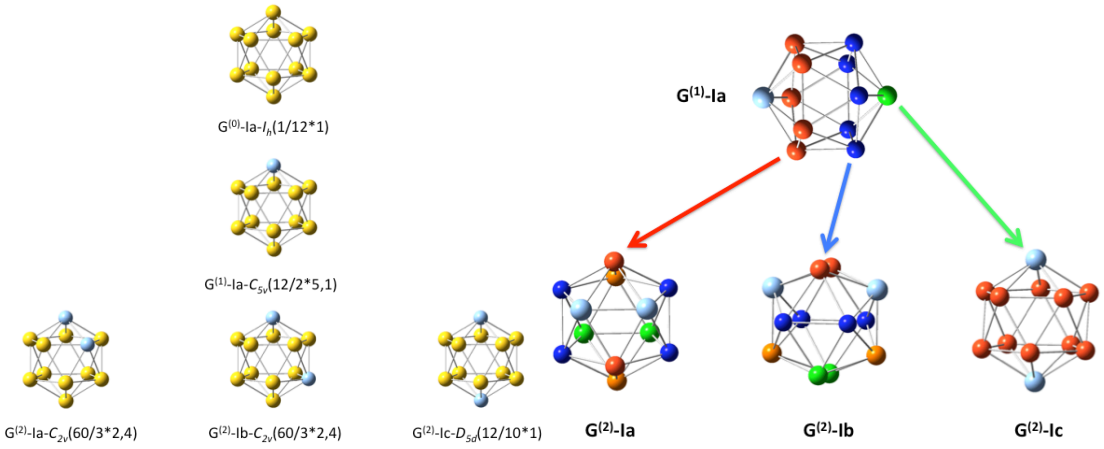

Figure 2. Left: Isomers in generations $G^{(0)}$, $G^{(1)}$, and $G^{(2)}$. Yellow, A; light blue, B. Right: Symmetry equivalencies in the individual isomers of $G^{(1)}$ and $G^{(2)}$. The equivalent atoms are highlighted in the same color. The single isomer of $G^{(1)}$ is shown at the top, and the three groups of symmetry equivalent atoms are highlighted in red,

dark blue, and green, respectively. The arrows point to the $G^{(2)}$-Isomers generated from substitution of one of these atoms in the respective group, as highlighted by the color of the arrows. The three isomers of $G^{(2)}$ are also colored according to the symmetry equivalency of the remaining ten atoms of A (red, dark blue, green, orange). Note that the isomers were rotated to enhance visibility.

From $G^{(2)}$, nine isomers can be constructed (which are in part equivalent, *vide infra*). From $G^{(2)}$-Ia, four isomers are formed (Table 4); $G^{(3)}$-I1, $G^{(3)}$-I2, $G^{(3)}$-I3, $G^{(3)}$-I4, and $G^{(3)}$-I5. These have degeneracies of 2*60, 2*60, 2*60, 2*60, and 4*60, respectively. From G(2)-Ib, another four isomers are formed ($G^{(3)}$-I5 to $G^{(3)}$-I8, with the same degeneracies as I1 – I4). From $G^{(2)}$-Ic, only one isomer, $G^{(3)}$-I9 (with degeneracy 120) is obtained. Careful inspection of these isomers shows that some are identical: $G^{(3)}$-I(5) = $G^{(3)}$-I4, $G^{(3)}$-I6 = $G^{(3)}$-I3, $G^{(3)}$-I8 = $G^{(3)}$-I2, and $G^{(3)}$-I9 = $G^{(3)}$-I3. Hence, only five distinguishable isomers are identified in $G^{(3)}$ (Figure 3, Table 5).

Table 4. Isomers generated in $G^{(3)}$.

Isomer	Parent Isomer	Identical to	Degeneracy	Point Group
$G^{(3)}$-I1	$G^{(2)}$-Ia	-	120	C_{3v}
$G^{(3)}$-I2	$G^{(2)}$-Ia	-	120	C_s
$G^{(3)}$-I3	$G^{(2)}$-Ia	-	120	C_s
$G^{(3)}$-I4	$G^{(2)}$-Ia	-	240	C_s
$G^{(3)}$-I5	$G^{(2)}$-Ib	$G^{(3)}$-I4	120	C_s
$G^{(3)}$-I6	$G^{(2)}$-Ib	$G^{(3)}$-I3	120	C_s
$G^{(3)}$-I7	$G^{(2)}$-Ib	-	120	C_{3v}
$G^{(3)}$-I8	$G^{(2)}$-Ib	$G^{(3)}$-I2	240	C_s
$G^{(3)}$-I9	$G^{(2)}$-Ic	$G^{(3)}$-I3	120	C_s

Table 5. Combined isomers in $G^{(3)}$ (A_9B_3), with degeneracies and full descriptor.

Isomer	Combined Isomers	Parent Isomer(s)	Rel. Degeneracy	Point group
$G^{(3)}$-Ia	$G^{(3)}$-I1	$G^{(2)}$-Ia	1	C_{3v}(120/3*3)
$G^{(3)}$-Ib	$G^{(3)}$-I2, $G^{(3)}$-I8	$G^{(2)}$-Ia, $G^{(2)}$-Ib	3	C_s(360/3*2, 3*1)
$G^{(3)}$-Ic	$G^{(3)}$-I3, $G^{(3)}$-I6, $G^{(3)}$-I9	$G^{(2)}$-Ia, $G^{(2)}$-Ib, $G^{(2)}$-Ic	3	C_s(360/4*2, 1*1)
$G^{(3)}$-Id	$G^{(3)}$-I4, $G^{(3)}$-I5	$G^{(2)}$-Ia, $G^{(2)}$-Ib	3	C_s(360/3*2, 3*1)
$G^{(3)}$-Ie	$G^{(3)}$-I7	$G^{(2)}$-Ib	1	C_{3v}(120/3*3)

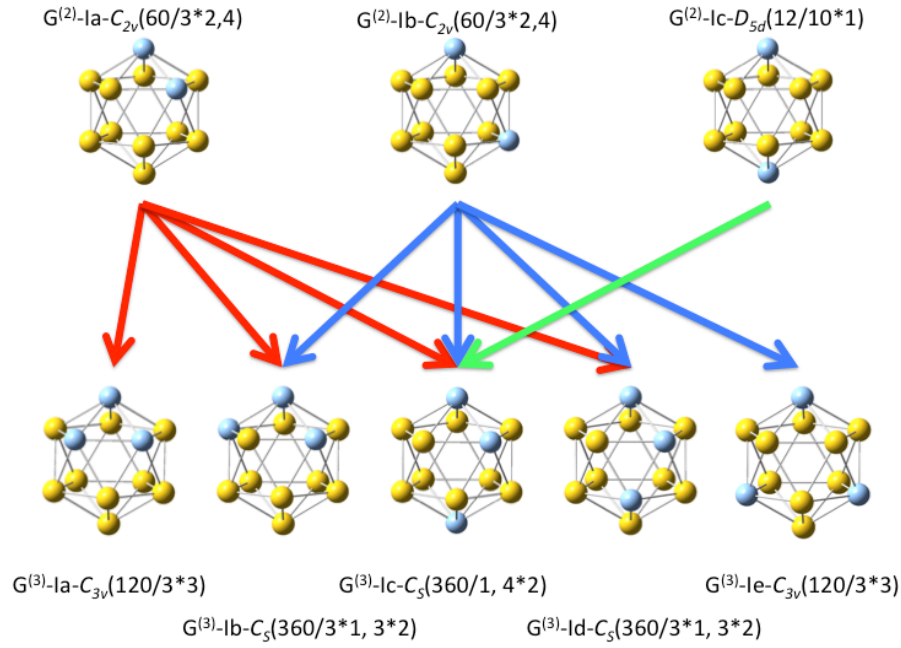

Figure 3. The five combined isomers in $G^{(3)}$ as obtained from the three isomers in $G^{(2)}$. The symmetry equivalencies in the $G^{(3)}$ isomers are not shown.

The construction of the isomers in the first three generations is fairly easy to follow, since only nine individual isomers can be constructed (in $G^{(3)}$) and have to be compared for equivalency (leading to five distinguished isomers). For $G^{(4)}$, however, this becomes much more complex. $G^{(3)}$-Ia and $G^{(3)}$-Ie have each three groups of equivalent atoms, $G^{(3)}$-Ib and $G^{(3)}$-Id have each six groups of equivalent atoms, and $G^{(3)}$-Ic has five groups of equivalent atoms. This leads to a total of 23 potential new isomers in $G^{(4)}$, which have to be compared for equivalency. These isomers are generated in the same way as the ones in $G^{(3)}$ from the ones in $G^{(2)}$. The process is not described in detail. After combination of equivalent isomers, ten possible isomers are found in $G^{(4)}$ (Figure 4, Table 6). For the first time, chiral isomers are found (two different chiral isomers are identified). Enantiomers are considered as identical. Five isomers have the point group C_s, two isomers are C_{2v}, another two are C_2 and the remaining isomer is D_{2h}.

Table 6. Isomers of $G^{(4)}$ (A_8B_4) with degeneracies.

Isomer	Parent Isomer(s)	Degeneracy	Point group
$G^{(4)}$-Ia	$G^{(3)}$-Ia, $G^{(3)}$-Id	2	C_{2v}(720/1*4, 2*2)
$G^{(4)}$-Ib	$G^{(3)}$-Ia, $G^{(3)}$-Ib, $G^{(3)}$-Id	4	C_s(1440/3*2, 2*1)
$G^{(4)}$-Ic	$G^{(3)}$-Ia, $G^{(3)}$-Ib, $G^{(3)}$-Ic	4	C_s(1440/3*2, 2*1)
$G^{(4)}$-Id	$G^{(3)}$-Ib, $G^{(3)}$-Ie	2	C_{2v}(720/1*4, 2*2)
$G^{(4)}$-Ie	$G^{(3)}$-Ib, $G^{(3)}$-Id	4	C_s(1440/2*2, 4*1)
$G^{(4)}$-If	$G^{(3)}$-Ib, $G^{(3)}$-Ic	4	C_2(1440/4*2)
$G^{(4)}$-Ig	$G^{(3)}$-Ib, $G^{(3)}$-Id, $G^{(3)}$-Ie	4	C_s(1440/3*2, 2*1)
$G^{(4)}$-Ih	$G^{(3)}$-Ic	1	D_{2h}(360/2*4)
$G^{(4)}$-Ii	$G^{(3)}$-Ic, $G^{(3)}$-Id, $G^{(3)}$-Ie	4	C_s(1440/3*2, 2*1)
$G^{(4)}$-Ij	$G^{(3)}$-Ic, $G^{(3)}$-Id	4	C_2(1440/4*2)

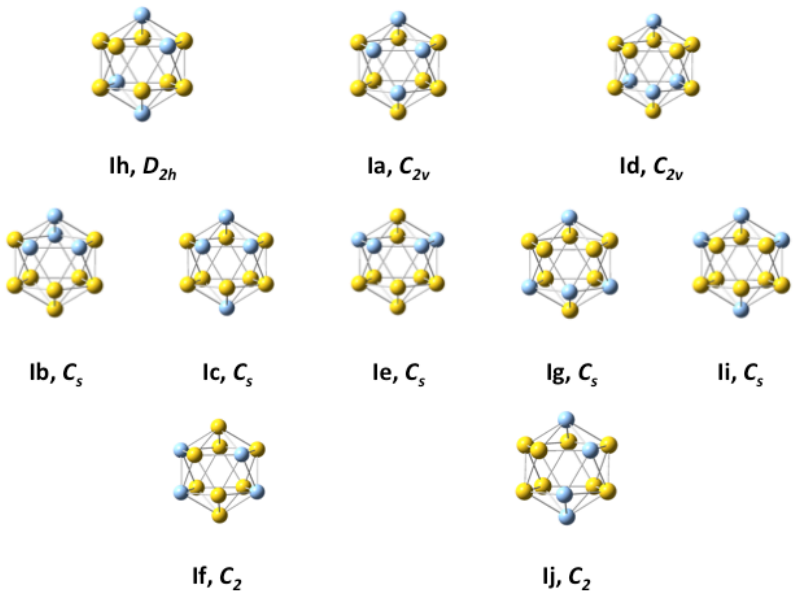

Figure 4. The ten isomers in $G^{(4)}$, grouped according to their symmetries. For details, see Table 6 and the text.

Analysis of the atom equivalency of the isomers in $G^{(4)}$ leads to a maximum of 42 isomers in $G^{(5)}$. It is expected that again a number of these isomers will be equivalent and that the number of actual isomers is lower. Indeed, the 42 possible isomers combine to twelve distinct isomers (Figure 5, Table 7). Two isomers are chiral with point group C_1, one isomer has the point group C_{5v}, and the remaining nine isomers are of C_s symmetry.

Table 7. Isomers of $G^{(5)}$ (A_7B_5) with degeneracies.

Isomer	Parent Isomer(s)	Rel. Degeneracy	Point group
$G^{(5)}$-Ia	$G^{(4)}$-Ia, $G^{(4)}$-Ib, $G^{(4)}$-Ie	5	C_s(7200/2*2, 3*1)
$G^{(5)}$-Ib	$G^{(4)}$-Ia, $G^{(4)}$-Ib, $G^{(4)}$-Ic, $G^{(4)}$-Ij	5	C_s(7200/3*2, 1*1)
$G^{(5)}$-Ic	$G^{(4)}$-Ia, $G^{(4)}$-Ic, $G^{(4)}$-Ig, $G^{(4)}$-Ii	5	C_s(7200/3*2, 1*1)
$G^{(5)}$-Id	$G^{(4)}$-Ib, $G^{(4)}$-Ic, $G^{(4)}$-Id, $G^{(4)}$-Ii	5	C_s(7200/3*2, 1*1)
$G^{(5)}$-Ie	$G^{(4)}$-Ib, $G^{(4)}$-Ic, $G^{(4)}$-Ie, $G^{(4)}$-If, $G^{(4)}$-Ij	10	C_1(14400/7*1)
$G^{(5)}$-If	$G^{(4)}$-Ib, $G^{(4)}$-Ie, $G^{(4)}$-Ig	5	C_s(7200/2*2, 3*1)
$G^{(5)}$-Ig	$G^{(4)}$-Ic, $G^{(4)}$-If, $G^{(4)}$-Ih	5	C_s(7200/2*2, 3*1)
$G^{(5)}$-Ih	$G^{(4)}$-Id, $G^{(4)}$-Ie, $G^{(4)}$-Ig	5	C_s(7200/2*2, 3*1)
$G^{(5)}$-Ii	$G^{(4)}$-Id, $G^{(4)}$-If, $G^{(4)}$-Ig, $G^{(4)}$-Ii	5	C_s(7200/3*2, 1*1)
$G^{(5)}$-Ij	$G^{(4)}$-Ie	1	C_{5v}(1440/1*5, 2*1)
$G^{(5)}$-Ik	$G^{(4)}$-Ie, $G^{(4)}$-If, $G^{(4)}$-Ig, $G^{(4)}$-Ii, $G^{(4)}$-Ij	10	C_1(14400/7*1)
$G^{(5)}$-Il	$G^{(4)}$-Ih, $G^{(4)}$-Ii, $G^{(4)}$-Ij	5	C_s(7200/2*2, 3*1)

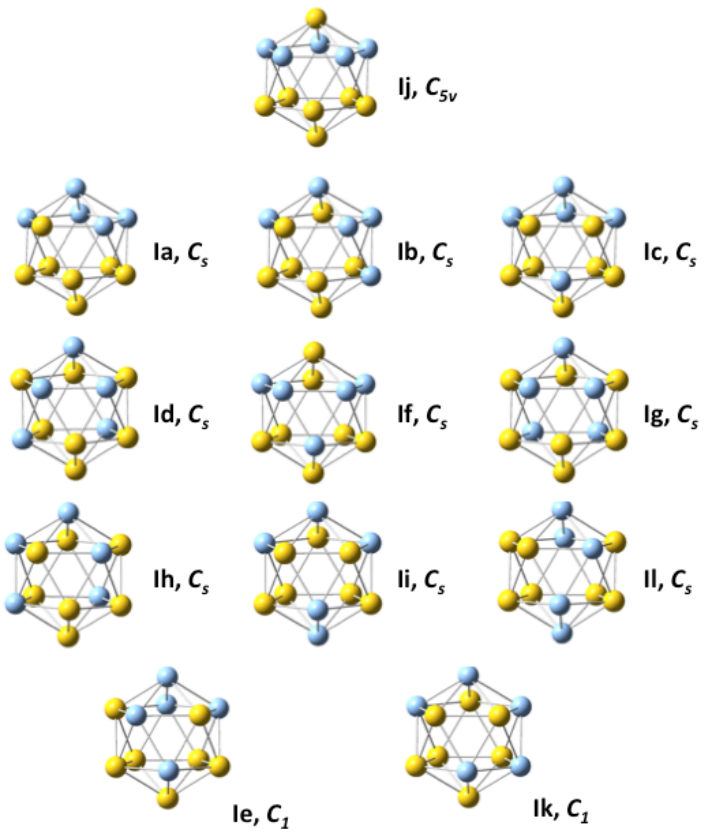

Figure 5. Isomers in $G^{(5)}$ grouped according to their point groups. For details, see Table 7 and the text.

For $G^{(6)}$, up to 58 isomers can be constructed, of which some will be equivalent. After combination, 18 distinct isomers are identified (Figure 6, Table 8). Of these, six have chiral point groups (four times C_1 and two times C_2). Higher symmetries are found in D_{3d} (two times), C_{2v} (four times), C_{3v} (two times) and C_{5v} (two times), and C_s (two times). It is obvious that the isomers obtained in $G^{(6)}$ already contain the complementary ones. This is most evident for the D_{3d} structures, which can be thought of as A_6 (B_6) rings in a chair conformation (analogous to cyclohexane) which is capped by two B_3 (A_3) rings above and below the planes. These are isomers $G^{(6)}$-In and $G^{(6)}$-Ir, respectively. In some cases, the complementary isomer is identical to the original one (e.g. in the C_{5v} cases).

Table 8. Isomers of $G^{(6)}$ (A_6B_6) with degeneracies.

Isomer	Parent Isomer(s)	Rel. Degeneracy	Point group
$G^{(6)}$-Ia	$G^{(5)}$-Ia, $G^{(5)}$-Ij	6	C_{5v}(8640/1*5, 1*1)
$G^{(6)}$-Ib	$G^{(5)}$-Ia, $G^{(5)}$-If	10	C_{3v}(14400/2*3)
$G^{(6)}$-Ic	$G^{(5)}$-Ia, $G^{(5)}$-Ic, $G^{(5)}$-Id, $G^{(5)}$-Ih	30	C_s(43200/2*2, 2*1)
$G^{(6)}$-Id	$G^{(5)}$-Ia, $G^{(5)}$-Ib, $G^{(5)}$-Ie	30	C_2(43200/3*2)
$G^{(6)}$-Ie	$G^{(5)}$-Ia, $G^{(5)}$-Ib, $G^{(5)}$-Ic, $G^{(5)}$-Ie, $G^{(5)}$-If, $G^{(5)}$-Ik	60	C_1(86400/6*1)
$G^{(6)}$-If	$G^{(5)}$-Ib, $G^{(5)}$-Id, $G^{(5)}$-Il	15	C_{2v}(21600/1*4, 1*2)
$G^{(6)}$-Ig	$G^{(5)}$-Ib, $G^{(5)}$-Ic, $G^{(5)}$-Ie, $G^{(5)}$-Ig, $G^{(5)}$-Ik, $G^{(5)}$-Il	60	C_1(86400/6*1)
$G^{(6)}$-Ih	$G^{(5)}$-Ic, $G^{(5)}$-Ig, $G^{(5)}$-Ie	15	C_{2v}(21600/1*4, 1*2)
$G^{(6)}$-Ii	$G^{(5)}$-Id, $G^{(5)}$-Ie, $G^{(5)}$-Ig, $G^{(5)}$-Ii, $G^{(5)}$-Ik, $G^{(5)}$-Il	60	C_1(86400/6*1)
$G^{(6)}$-Ij	$G^{(5)}$-Id, $G^{(5)}$-Ie, $G^{(5)}$-If, $G^{(5)}$-Ih, $G^{(5)}$-Ii, $G^{(5)}$-Ik	60	C_1(86400/6*1)
$G^{(6)}$-Ik	$G^{(5)}$-Ie, $G^{(5)}$-If, $G^{(5)}$-Ij, $G^{(5)}$-Ik	30	C_s(43200/2*2, 2*1)
$G^{(6)}$-Il	$G^{(5)}$-Ie, $G^{(5)}$-Ig	15	C_{2v}(21600/3*2)
$G^{(6)}$-Im	$G^{(5)}$-If, $G^{(5)}$-Ih	10	C_{3v}(14400/2*3)
$G^{(6)}$-In	$G^{(5)}$-Ig	5	D_{3d}(7200/1*6)
$G^{(6)}$-Io	$G^{(5)}$-Ih, $G^{(5)}$-Ij	6	C_{5v}(8640/1*5, 1*1)
$G^{(6)}$-Ip	$G^{(5)}$-Ih, $G^{(5)}$-Ii, $G^{(5)}$-Ik	30	C_2(43200/3*2)
$G^{(6)}$-Iq	$G^{(5)}$-Ik, $G^{(5)}$-Il	15	C_{2v}(21600/3*2)
$G^{(6)}$-Ir	$G^{(5)}$-Il	5	D_{3d}(7200/1*6)

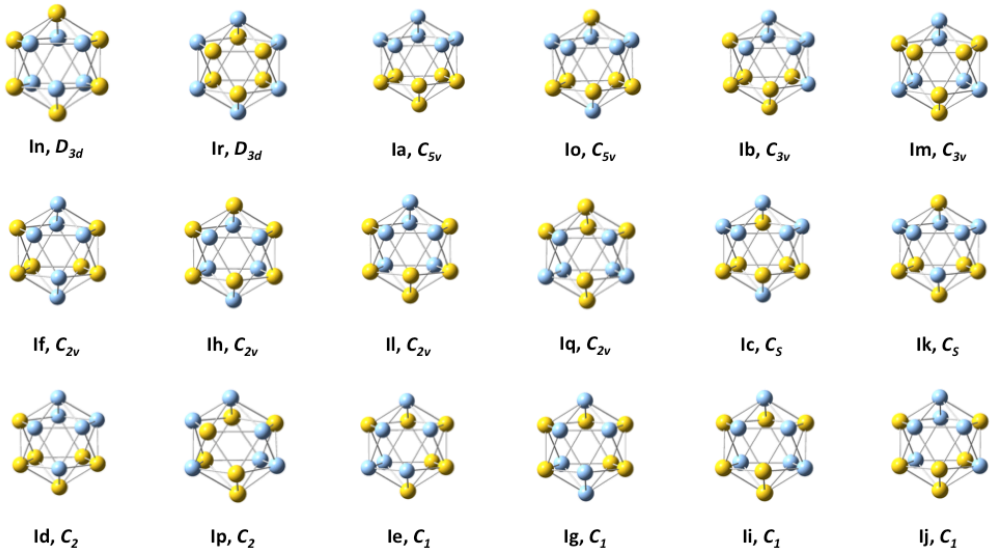

Figure 6. Isomers of $G^{(6)}$ grouped according to their point group symmetries (the chiral isomers are shown in the bottom row).

All isomers derived from A_{12} have point groups that are sub-groups of I_h. This indicates that with each substitution, the symmetry of the parent isomer is lowered. This, however, is not the case. In fact, a low symmetry isomer may lead to one of high symmetry when substituting appropriately. For instance, $G^{(6)}$-Ih (C_{2v}) is a derivative of $G^{(5)}$-Ie (C_1). Therefore, one must consider that these relationships apply in both directions: A high symmetry isomer may be obtained from a low symmetry isomer, and a low symmetry isomer may be obtained from a high symmetry isomer. Also, inspection of the point groups and their relation to their parent isomers or their offsprings reveals that there is not always a direct relation between their point groups. For instance, $G^{(2)}$-Ia (C_{2v}) leads to $G^{(3)}$-Ia with C_{3v} symmetry. The C_{3v} point group is not a subgroup of the C_{2v} point group (or *vice versa*). One has to consider that in this case the principal axes of the point groups are not the same. While in the C_{2v} case, the principal axis falls into the center of the B-B bond, a B-B-B triangle is formed in the C_{3v} case. The principal axis is then moved into the center of this triangular face. If the original C_2 axis were used for reference, C_1 symmetry would be obtained (and C_1 is a subgroup of C_{2v}).

Chirality is an important property in chemistry. This spans over applications of chiral clusters in asymmetric catalysis or their use in nonlinear optics, especially second-order processes which are dominated by the molecular symmetry. Second-order scattering requires the absence of centrosymmetry, and chirality effectively ensures

this absence. Beginning with A_8B_4, chiral geometries are obtained. This is intuitively clear, since four points in three dimensions can be arranged in helical fashion, whereas three points always form a plane. In A_7B_5 and A_6B_6, chirality is much more likely to be found than in the other structures. Comparison of the degeneracies shows that in $G^{(4)}$ the relative weight of chiral point groups to achiral one is 8:25 (0.32), in $G^{(5)}$ this increases to 20:46 (ca. 0.435) and in $G^{(6)}$, a chiral:achiral ratio of 300:162 (1.85). Since A_5B_7 and A_4B_8 are equivalent to A_7B_5 and A_8B_4, the center of the distribution (ranging from $A_{12}B_0$ to A_0B_{12}) marks the range in which chirality may be present. It should be noted that this fact does not necessarily reflect a realistic situation, since the relative energies of the isomers have to be taken into account.
It is particularly difficult to identify and compare the isomers of C_1 symmetries. In the $G^{(6)}$ isomers, four of these are found, and there a simple way to compare the isomers. In each of the structures, at least four of the B-atoms (or the A-atoms) form a chain and can be represented to lie in one plane of the icosahedron (by appropriate rotation). From this B_4-chain, the remaining two atoms are placed in the upper plane. The positions of the remaining two B-atoms define the isomer, and the pattern has to be different for each isomer (Figure 7).

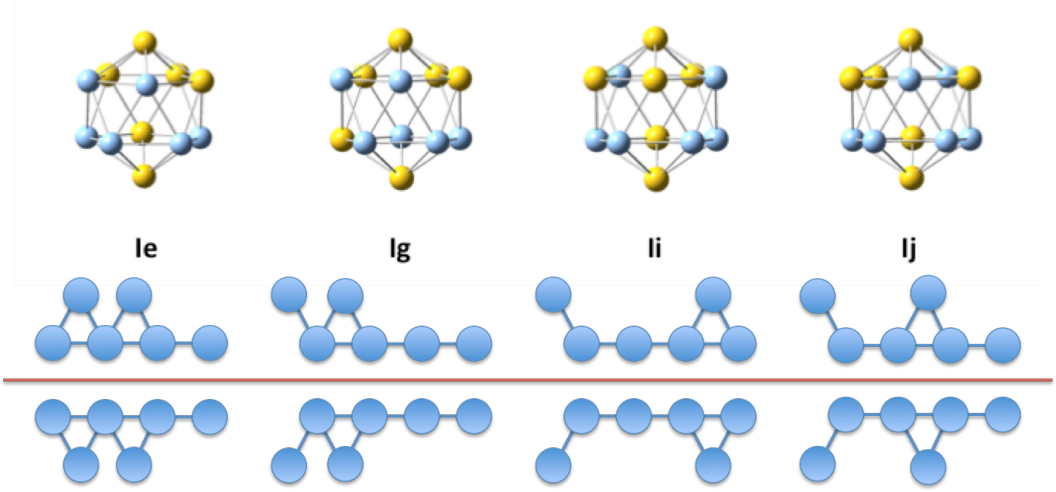

Figure 7. Chirality highlighted in the C_1 isomers of $G^{(6)}$. At the bottom, the connectivity of the B-atoms in each C_1 isomer and their respective enantiomer is shown, separated by the red line.

The algorithm used here to generate the isomers of the (quasi-)icosahedral $A_{12-x}B_x$ clusters can in principle be applied to all kinds of clusters. A high starting geometry

and atom equivalency is desirable, however. This immediately becomes obvious when inspecting the tetrahedral Au_{20} cluster, which shall be outlined here.[36] The monometallic cluster has the point group T_d, but not all the atoms are symmetry equivalent. They split in three sets consisting of four, twelve and four atoms (which are the vertices, the atoms on the edges and the atoms on the faces of the tetrahedron). Thus, there are already three isomers in $G^{(1)}$, of C_{3v}, C_s and C_{3v} geometry, respectively (Figure 8). In the C_s isomer, no less than twelve distinct symmetry environments for the remaining atoms of A are identified. This may highlight the high number of potential isomers that may arise in the construction of binary clusters if the starting geometry already bears different symmetry environments.

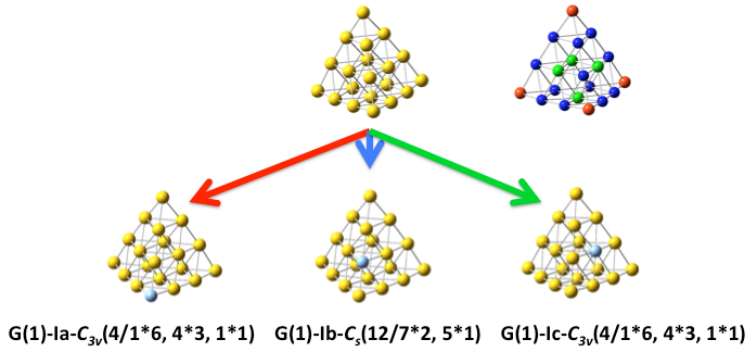

Figure 8. $G^{(0)}$ and $G^{(1)}$ of the (quasi-)tetrahedral $A_{20-x}B_x$ clusters. Due to the non-degeneracy of the atoms in A_{20}, already three isomers are possible in $G^{(1)}$. At the top right, the atoms of A_{20} are colored according to their symmetry equivalency; the color of the arrows indicates the isomer formed by substitution of these.

Conclusion and Outlook

All possible isomers of (quasi-)icosahedral $A_{12-x}B_x$ (x = 0 – 6) were constructed using a symmetry-based algorithm, and their (relative) degeneracies are provided for reference. The number of possible isomers rises with each generation. Chirality is observed in A_8B_4, A_7B_5, and A_6B_6 (and A_5B_7, A_4B_8), which may be of relevance in designing materials for second-order nonlinear optical processes or asymmetric catalysts. The presented isomers are intended to provide a reference guide and stimulate research on binary metal clusters with higher substitution.

Overall, the algorithm serves as a general guideline for the construction of isomers in binary atomic or metal clusters, as well as for substituted ligand spheres in coordination compounds. While this is trivial for square-planar (ML_4), tetrahedral

(ML_4) or octahedral (ML_6) geometries, the problem becomes much more complicated in clusters which contain larger numbers of atoms to start from. This was demonstrated for the icosahedral system. In the tetrahedral A_{20} cluster, already the first generation $A_{19}B_1$ has three distinct isomers, which leads to a high number of isomers in the second generation, $A_{18}B_2$.

Acknowledgment

The author thanks KU Leuven and the German Academic Exchange Service (DAAD) for financial support. Useful discussions with Ward Brullot, Maarten Bloemen, and Thierry Verbiest (all KU Leuven) are acknowledged.

Supplementary Information

Coordinates of the $G^{(3)}$ – $G^{(6)}$ isomers of $A_{12-x}B_x$.

References

[1] A.W. Castleman, S.N. Khanna, Clusters, Superatoms, and Building Blocks of New Materials†, J. Phys. Chem. C. 113 (2009) 2664–2675. doi:10.1021/jp806850h.

[2] H. Häkkinen, Atomic and electronic structure of gold clusters: understanding flakes, cages and superatoms from simple concepts., Chem. Soc. Rev. 37 (2008) 1847–1859. doi:10.1039/b717686b.

[3] R. Jin, Atomically precise metal nanoclusters: stable sizes and optical properties, Nanoscale. 7 (2015) 1549–1565. doi:10.1039/C4NR05794E.

[4] T. Tsukuda, Toward an Atomic-Level Understanding of Size-Specific Properties of Protected and Stabilized Gold Clusters, Bull. Chem. Soc. Jpn. 85 (2012) 151–168. doi:10.1246/bcsj.20110227.

[5] V. Marjomaki, T. Lahtinen, M. Martikainen, J. Koivisto, S. Malola, K. Salorinne, et al., Site-specific targeting of enterovirus capsid by functionalized monodisperse gold nanoclusters, Proc Natl Acad Sci U S A. 111 (2014) 1277–1281. doi:10.1073/pnas.1310973111.

[6] J.F. Hainfeld, D.N. Slatkin, T.M. Focella, H.M. Smilowitz, Gold nanoparticles: a new X-ray contrast agent, Br J Radiol. 79 (2006) 248–253. doi:10.1259/bjr/13169882.

[7] L.-Y. Chen, C.-W. Wang, Z. Yuan, H.-T. Chang, Fluorescent Gold Nanoclusters: Recent Advances in Sensing and Imaging, Anal. Chem. 87 (2015) 216–229. doi:10.1021/ac503636j.

[8] S. Knoppe, M.K. Vanbel, S.J. Van Cleuvenbergen, L. Vanpraet, T. Burgi, T. Verbiest, Nonlinear Optical Properties of Thiolate-Protected Gold Clusters, J. Phys. Chem. C. 119 (2015) 6221 – 6226. doi:10.1021/acs.jpcc.5b01475.

[9] A. Sanchez, S. Abbet, U. Heiz, W.D. Schneider, H. Häkkinen, R.N. Barnett, et al., When Gold Is Not Noble: Nanoscale Gold Catalysts, J. Phys. Chem. A. 103 (1999) 9573–9578. doi:10.1021/jp9935992.

[10] Y. Zhu, H.F. Qian, R.C. Jin, Catalysis opportunities of atomically precise gold nanoclusters, J. Mater. Chem. 21 (2011) 6793–6799. doi:Doi 10.1039/C1jm10082c.

[11] Y. Negishi, W. Kurashige, Y. Niihori, K. Nobusada, Toward the creation of stable, functionalized metal clusters, Phys Chem Chem Phys. 15 (2013) 18736–18751. doi:10.1039/c3cp52837e.

[12] C. Kumara, C.M. Aikens, A. Dass, X-ray Crystal Structure and Theoretical Analysis of Au25–xAgx(SCH2CH2Ph)18–Alloy, J. Phys. Chem. Lett. 5 (2014) 461–466. doi:10.1021/jz402441d.

[13] M.W. Heaven, A. Dass, P.S. White, K.M. Holt, R.W. Murray, Crystal structure of the gold nanoparticle [N(C8H17)4][Au25(SCH2CH2Ph)18], J Am Chem Soc. 130 (2008) 3754–3755. doi:10.1021/ja800561b.

[14] M. Walter, M. Moseler, Ligand-protected gold alloy clusters: Doping the superatom, J. Phys. Chem. C. 113 (2009) 15834–15837. doi:10.1021/jp9023298.

[15] D.R. Kauffman, D. Alfonso, C. Matranga, H. Qian, R. Jin, A Quantum Alloy: The Ligand-Protected Au 25– x Ag x (SR) 18 Cluster, J. Phys. Chem. C. 117 (2013) 7914–7923. doi:10.1021/jp4013224.

[16] C. a. Fields-Zinna, M.C. Crowe, A. Dass, J.E.F. Weaver, R.W. Murray, Mass spectrometry of small bimetal monolayer-protected clusters, Langmuir. 25 (2009) 7704–7710. doi:10.1021/la803865v.

[17] M.J. Hartmann, H. Häkkinen, J.E. Millstone, D.S. Lambrecht, Impacts of Copper Position on the Electronic Structure of [Au 25-x Cu x (SH) 18] − Nanoclusters, J. Phys. Chem. C. 119 (2015) 8290–8298. doi:10.1021/jp5125475.

[18] B.K. Teo, K. Keating, Novel triicosahedral structure of the largest metal alloy cluster: hexachlorododecakis(triphenylphosphine)-gold-silver cluster

[(Ph3P)12Au13Ag12Cl6]m+, J. Am. Chem. Soc. 106 (1984) 2224–2226. doi:10.1021/ja00319a061.

[19] B.K. Teo, M.C. Hong, H. Zhang, D.B. Huang, Cluster of Clusters: Structure of the 37-Atom Cluster[(p-Tol3P)12Au18Ag19Br11]2⊕ and a Novel Series of Supraclusters Based on Vertex-Sharing Icosahedra, Angew. Chemie Int. Ed. English. 26 (1987) 897–900. doi:10.1002/anie.198708971.

[20] B.K. Teo, H. Zhang, X. Shi, Molecular architecture of a novel vertex-sharing biicosahedral cluster [(p-Tol3P)10Au13Ag12Br8](PF6) containing a staggered-staggered-staggered configuration for the 25-atom metal framework, Inorg. Chem. 29 (1990) 2083–2091. doi:10.1021/ic00336a011.

[21] C. Kumara, K.J. Gagnon, A. Dass, X-ray Crystal Structure of Au38–xAgx(SCH2CH2Ph)24 Alloy Nanomolecules, J. Phys. Chem. Lett. 6 (2015) 1223–1228. doi:10.1021/acs.jpclett.5b00270.

[22] T. Verbiest, K. Clays, V. Rodríguez, Second-order Nonlinear Optical Characterization Techniques: An Introduction, 1st ed., CRC Press, n.d.

[23] D.E. Bergeron, a W. Castleman, T. Morisato, S.N. Khanna, Formation of Al13I-: evidence for the superhalogen character of Al13., Science. 304 (2004) 84–87. doi:10.1126/science.1093902.

[24] O.P. Charkin, D.O. Charkin, N.M. Klimenko, A.M. Mebel, A theoretical study of isomerism in doped aluminum MAl12 and MAl12X12 clusters with 40 and 50 valence electrons., Faraday Discuss. 124 (2003) 215–237; discussion 275–288, 453–455. doi:10.1039/b211114d.

[25] X. Gong, V. Kumar, Enhanced stability of magic clusters: A case study of icosahedral Al12X, X=B, Al, Ga, C, Si, Ge, Ti, As, Phys. Rev. Lett. 70 (1993) 2078–2081. doi:10.1103/PhysRevLett.70.2078.

[26] E. Jimenez-Izal, D. Moreno, J.M. Mercero, J.M. Matxain, M. Audiffred, G. Merino, et al., Doped Aluminum Cluster Anions: Size Matters, J. Phys. Chem. A. 118 (2014) 4309–4314. doi:10.1021/jp501496b.

[27] R. Pal, L.-F. Cui, S. Bulusu, H.-J. Zhai, L.-S. Wang, X.C. Zeng, Probing the electronic and structural properties of doped aluminum clusters: MAl12-(M=Li, Cu, and Au)., J. Chem. Phys. 128 (2008) 024305. doi:10.1063/1.2805386.

[28] Z. Chen, G. Wang, X. Zhao, A. Tang, Isomerism and aromaticity of heterofullerene C 70- n P n (n =2-10), J. Mol. Model. 8 (2002) 223–229. doi:10.1007/s00894-002-0090-0.

[29] Z. Chen, U. Reuther, A. Hirsch, W. Thiel, Theoretical Studies on the Substitution Patterns in Heterofullerenes $C_{70-x}N_x$ and $C_{70-x}B_x$ (x = 2−10), J. Phys. Chem. A. 105 (2001) 8105–8110. doi:10.1021/jp0118773.

[30] J. Pattanayak, T. Kar, S. Scheiner, Boron−Nitrogen (BN) Substitution Patterns in C/BN Hybrid Fullerenes: $C_{60-2x}(BN)_x$ (x = 1−7), J. Phys. Chem. A. 105 (2001) 8376–8384. doi:10.1021/jp011391m.

[31] J. Pattanayak, T. Kar, S. Scheiner, Boron-nitrogen (BN) substitution of fullerenes: C60 to C12B24N24 CBN ball, J. Phys. Chem. A. 106 (2002) 2970–2978. doi:10.1021/jp013904v.

[32] Z. Chen, K. Ma, Y. Pan, X. Zhao, A. Tang, (X = N, B), Can. J. Chem. 77 (1999) 291–298. doi:10.1139/v99-016.

[33] B.F.G. Johnson, A.W. Bott, D. Hugh-Jones, A. Rodger, Geometrical and orientational isomers in clusters, Polyhedron. 9 (1990) 1769–1774. doi:10.1016/S0277-5387(00)83986-8.

[34] R. Grimes, Carboranes, 1st Editio, Academic Press, New York, 1970.

[35] R.F. Trimble, Isomers of octahedral complexes with nonbranching ligands, J. Chem. Educ. 31 (1954) 176. doi:10.1021/ed031p176.

[36] J. Li, X. Li, H.J. Zhai, L.S. Wang, Au20: a tetrahedral cluster, Science (80-.). 299 (2003) 864–867. doi:10.1126/science.1079879.